Magnetization reversal and interlayer coupling in Co 50 Fe 50 nanomagnets

V. Satya Narayana Murthy, C. Krishnamoorthi, R. Mahendiran, and A. O. Adeyeye

Citation: Journal of Applied Physics **105**, 023916 (2009); doi: 10.1063/1.3072624
View online: http://dx.doi.org/10.1063/1.3072624
View Table of Contents: http://scitation.aip.org/content/aip/journal/jap/105/2?ver=pdfcov
Published by the AIP Publishing

Magnetization reversal and interlayer coupling in $Co_{50}Fe_{50}$ nanomagnets

V. Satya Narayana Murthy,[1] C. Krishnamoorthi,[2] R. Mahendiran,[2] and A. O. Adeyeye[1,a)]
[1]*Department of Electrical and Computer Engineering, Information Storage Materials Laboratory, National University of Singapore, 4 Engineering Drive 3, Singapore 117576, Singapore*
[2]*Department of Physics, National University of Singapore, 2 Science Drive 3, Singapore 117542, Singapore*

(Received 23 October 2008; accepted 8 December 2008; published online 28 January 2009)

We investigated magnetization reversal mechanism in elliptical shaped nanomagnets made from single layer and pseudospin valve $Co_{50}Fe_{50}$ films. The structures were fabricated using deep ultraviolet lithography and the lift-off process. We observed that the magnetization reversal process of the single layer elements is strongly dependent on the film thickness. For thickness $t_{CoFe}=10$ nm, the magnetization reversal process is dominated by a systematic coherent rotation, whereas for $t_{CoFe}=60$ nm, the reversal process is mediated by vortex nucleation, displacement, and annihilation. By exploiting the thickness dependence of the magnetization reversal process, pseudospin valve nanomagnets from two $Co_{50}Fe_{50}$ thicknesses (10 and 60 nm) were fabricated. We also investigated the effect of interlayer exchange coupling in pseudospin valve structures by varying the Cu spacer layer (t_{Cu}). For $t_{Cu}\leq 5$ nm, the two ferromagnetic layers are found to be strongly coupled by exchange interaction. The strength of the coupling is significantly dependent on temperature. For $t_{Cu}\geq 20$ nm, the two $Co_{50}Fe_{50}$ layers are antiferromagnetically coupled at 300 K. As the temperature is reduced below 50 K, we observed a clear transition from antiferromagnetic to ferromagnetic coupling. © *2009 American Institute of Physics*. [DOI: 10.1063/1.3072624]

I. INTRODUCTION

Patterned magnetic nanostructures attracted considerable interest due to their potential applications in nonvolatile magnetic random access memory.[1,2] For low dimensional magnetic structures, the switching characteristics strongly depend on the shape and size. The influence of shape and size on the magnetic properties have been studied widely in nanomagnets, namely, square,[2,3] diamond,[4] triangular,[5] elliptical,[6,7] circular,[8] and ring.[9]

Patterned magnetic pseudospin valve (PSV) nanostructures in which two ferromagnetic (FM) layers separated by a nonmagnetic spacer layer have potential application in magnetoelectronic devices. From a fundamental viewpoint, the strong coupling between the various layers within the elements would lead to a variety of possible interesting magnetization states. Interlayer exchange coupling (IEC) is considered as one of the most crucial parameters to physically evaluate giant magnetoresistance for spintronic device applications.[10] IEC between the FM layers oscillates between FM and antiferromagnetic with the thickness of the spacer layer and the coupling strength decreasing with the increase in spacer layer thickness.[11] IEC has been studied in trilayers, multilayers, and wedge shaped trilayer structures with metal,[10–12] insulator,[13] semimetal,[14] and amorphous[15] layers as spacers between the FM layers.

Previously, Buchanan *et al.*[16] conducted detailed investigations on the magnetization reversal in patterned trilayer $Ni_{80}Fe_{20}/Cu/Ni_{80}Fe_{20}$ nanodots. Their experimental and numerical magnetic susceptibilities are in agreement with analytical calculations based on the rigid vortex model. The field dependence of the spin wave excitation in $Ni_{80}Fe_{20}/Cu/Ni_{80}Fe_{20}$ trilayered dots has also been investigated by Brillouin light scattering.[17] Recently, numerical simulations of the effects of interlayer interactions on the magnetization dynamics of a trilayer square element with the Landau domain structure has been investigated.[18] Castaño *et al.*[19] studied the magnetization reversal of sub-100-nm rectangular PSV structures and observed that the aspect ratio strongly influences the switching field. The interlayer coupling and magnetization reversal of Co/Au/Ni nanomagnets of different shapes including diamond was also investigated by Smith *et al.*[20] using off-axis electron holography technique and visually observed the antiferromagnetic coupling between the FM layers.

In this work we investigated in a systematic way the magnetization reversal process in $Co_{50}Fe_{50}$ as a function of thickness in elliptical nanostructures. The PSVs were fabricated with $Co_{50}Fe_{50}$ layers of two different thicknesses. We probed the interlayer exchange between the $Co_{50}Fe_{50}$ layers by varying the thickness of the Cu spacer layer in the range from 2 to 30 nm. We also investigated the effect of temperature on the reversal mechanism of ferromagnetically coupled ($t_{Cu}=2$ nm) and antiferromagnetically coupled ($t_{Cu}=20$ nm) PSVs. Micromagnetic simulations were performed to validate the reversal mechanism of the individual $Co_{50}Fe_{50}$ layers and the coupling between them.

II. EXPERIMENTAL DETAILS

Large area elliptical patterned nanostructures were fabricated on commercially available Si substrates using deep ultraviolet lithography at 248 nm wavelength. The details of the fabrication process are discussed in Ref. 21. The $Co_{50}Fe_{50}$ films with thicknesses of 10 and 60 nm were de-

a)Author to whom correspondence should be addressed. Electronic mail: eleaao@nus.edu.sg.

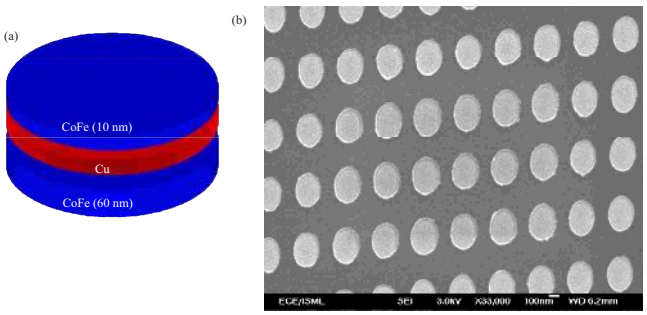

FIG. 1. (Color online) (a) Schematic of $Co_{50}Fe_{50}$(60 nm)/Cu/$Co_{50}Fe_{50}$(10 nm) elliptical PSV nanomagnet and (b) SEM of an array of elliptical $Co_{50}Fe_{50}$(60 nm)/Cu(20 nm)/$Co_{50}Fe_{50}$(10 nm)/Cu(5 nm) nanomagnet.

posited using electron beam evaporation technique. For the PSV structures, the two magnetic layer thicknesses were fixed at 10 and 60 nm, while the Cu spacer layer thickness is varied from 2 to 20 nm. Figure 1(a) shows a schematic of an elliptical PSV nanomagnet. Both the $Co_{50}Fe_{50}$ and Cu were deposited in the same electron beam deposition chamber with a base pressure of 1×10^{-7} torr at a rate of 0.4 Å/s. During film deposition, a blank Si substrate was placed in the chamber and used as the reference film. To prevent the oxidation of magnetic layers, the films were capped with a 5 nm Cu layer. Scanning electron micrograph (SEM) of elliptical $Co_{50}Fe_{50}$(60 nm)/Cu(20 nm)/$Co_{50}Fe_{50}$(10 nm)/Cu(5 nm) PSV nanomagnet array is shown in Fig. 1(b). The nanostructures are uniform and identical over a very large area. Their major and minor axes are 335 and 225 nm, respectively, and the separations between the nanostructures along the major and minor axes are 290 and 150 nm, respectively. Magnetization measurements were performed using a commercial vibrating sample magnetometer (Quantum Design Inc.) from room temperature down to 5 K.

III. RESULTS AND DISCUSSIONS

A. Single layer $Co_{50}Fe_{50}$ elliptical nanomagnets

Figure 2(a) shows the magnetic hysteresis loop variation along the major axis for two different thicknesses of $Co_{50}Fe_{50}$ films. The magnetization reversal is sensitive to the thickness of the $Co_{50}Fe_{50}$ nanomagnets. The observed remanence is high and the saturation field is low for 10 nm compared with the 60 nm nanomagnets. This is due to the characteristic of the magnetization reversal process being mediated by coherent rotation in the 10 nm nanomagnets.[22] The 60 nm nanomagnets displays an interesting variation in hysteresis loop. In contrast with 10 nm nanomagnets, the magnetization decreases rapidly at H_n before remanence. This rapid loss of net magnetization is continued up to H_1, which indicates the nucleation of the vortex states at H_n.[7,16,23] For fields $>H_1$, magnetization decreases slowly until remanence. A flux closure configuration (vortex) is formed at remanence, which lowers the energy of the system by minimizing the magnetostatic energy. In the positive direction of the field, the magnetization increases slowly until H_2. The linear region between H_1 and H_2 indicates the propagation of the vortex inside the ellipse. Above H_2 magnetization

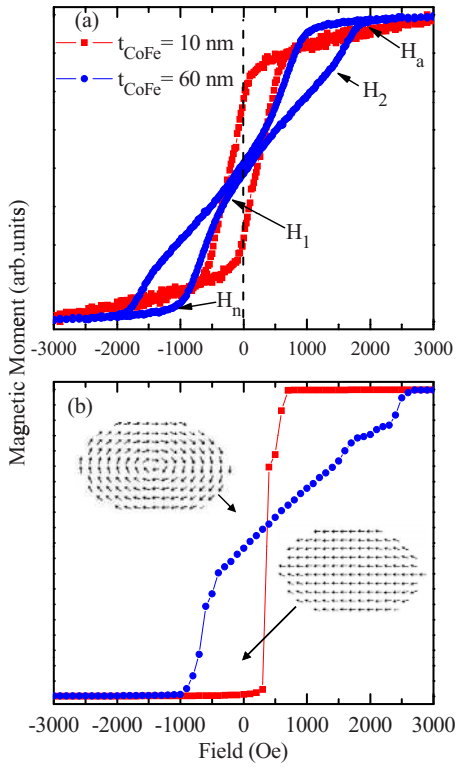

FIG. 2. (Color online) Magnetization loops of $Co_{50}Fe_{50}$ elliptical nanomagnetic arrays: (a) experimental and (b) simulated.

increases rapidly and annihilation of vortex states takes place at H_a. In order to understand the thickness dependence of the magnetization reversal process in nanomagnets, micromagnetic simulations were carried out by using object oriented micromagnetic framework (OOMMF) code from the National Institute of Standards and Technology.[24] The material parameters used in the simulations are saturation magnetization $M_s=1.9\times10^6$ A/m, exchange constant $A=3\times10^{-11}$ J/m, and anisotropy constant $K_1=0$ J/m^3.[25] The size of the cubic unit cell used is 5 nm. We assumed that the intrinsic uniaxial anisotropy of the bulk $Co_{50}Fe_{50}$ film is negligible when compared with the shape-induced anisotropy of the nanomagnets. The shape of the rings in the simulations was based on masks made from SEM images.

The simulations were performed by first saturating the nanomagnets along the major axis in the negative field direction. Figure 2(b) shows the magnetization curves generated by the simulations of 10 and 60 nm thick elliptical nanomagnets. The comparison of the experimental and simulated curves displays the same field behavior with some minor differences in switching fields and remanence. These differences may be accounted by thermal fluctuations, magnetostatic interactions between the neighboring nanomagnets, and the switching field distribution.[26] The remanent state configurations were captured in order to better understand the thickness dependent magnetization reversal mechanism in the elliptical shaped nanomagnets. Single domain configuration was observed in the case of 10 nm nanomagnets and vortex state was observed in 60 nm nanomagnets.

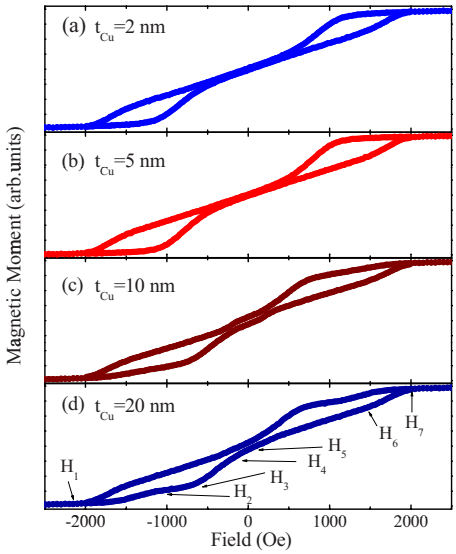

FIG. 3. (Color online) Magnetization loops of PSV elliptical nanomagnets for fields applied along the major axis as a function of Cu spacer layer at room temperature.

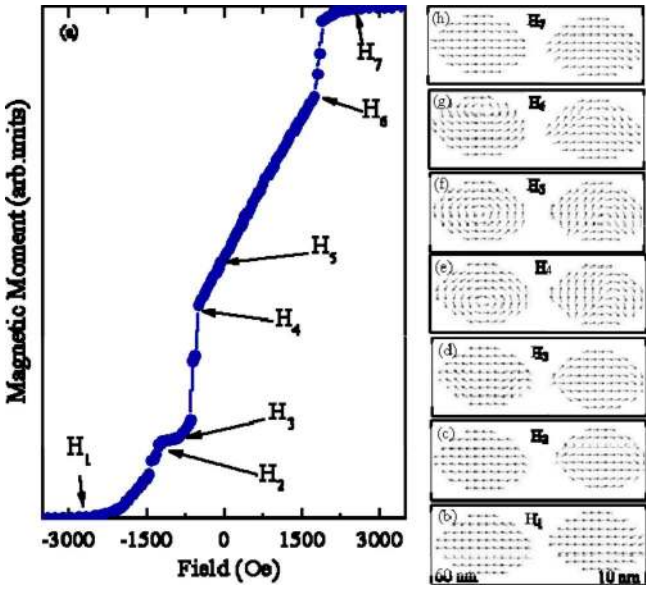

FIG. 4. (Color online) (a) Simulated magnetization loop of $Co_{50}Fe_{50}$(60 nm)/Cu(20 nm)/$Co_{50}Fe_{50}$(10 nm)/Cu(5 nm) PSV elliptical nanomagnets. The corresponding magnetic states of 60 and 10 nm $Co_{50}Fe_{50}$ layers are shown in (b)–(h).

B. Effect of Cu spacer layer thickness

Figure 3 shows the *M-H* loops for the PSV nanomagnets as a function of Cu spacer layer thickness for fields applied along the major axis at room temperature. As the spacer layer thickness increases, there is a change in the shape of the magnetic hysteresis loop. The variation in the *M-H* loop for t_{Cu}=2 and 5 nm is similar to that of the single layer $Co_{50}Fe_{50}$ nanomagnets 60 nm thick [Fig. 2(a)], suggesting that two systems are strongly coupled. When t_{Cu}=10 nm, the shape of the magnetic hysteresis loop changes slightly indicating a change in the coupling mechanism between the two FM layers. The strong FM coupling in t_{Cu}=2 and 5 nm PSVs comes from IEC through the Cu spacer layer. For t_{Cu}=10 nm, there is a decrease in the nucleation field to −780 Oe (−1150 Oe for t_{Cu}=5 nm) and an increase in the remanent magnetization. This shows that the magnetization reversal in PSV is favoring independent reversal of the FM layers, due to the changes in the coupling between the layers. By increasing the thickness (t_{Cu}=20 nm), a markedly different reversal with clear two step magnetization is observed as shown in Fig. 3(d). Similar field dependent behavior is observed for t_{Cu}=30 nm PSV. This type of reversal process indicates a weak antiferromagnetic coupling between the two FM layers at low fields.

In order to understand the micromagnetic structure and the coupling behavior between the two FM layers, three-dimensional micromagnetic simulations were performed for a dot with t_{Cu}=20 nm. The material parameters used are same as in single layer $Co_{50}Fe_{50}$ simulations. The size of the unit cell used is $10\times10\times2$ nm^3 in the x, y, and z directions. The z direction is taken perpendicular to the plane of the nanomagnets. Figure 4(a) shows the magnetization curve generated by simulations of t_{Cu}=20 nm PSV.

The stable magnetic configurations obtained at various points on the simulated magnetization reversal curve are also shown in Fig. 4. The respective magnetic fields are marked on both the experimental [Fig. 3(d)] and simulated [Fig. 4(a)] curves. The field H_1 indicates the saturated state of PSV. The magnetic states of the individual FM layers in the saturated state are shown in Fig. 4(b). The magnetic moments in the FM layers are saturated in the negative field direction. As the field is increased from H_1 to H_2, the magnetization decreases monotonically due to the spin reorientation in the 10 nm $Co_{50}Fe_{50}$ layer to decrease the magnetostatic energy of the system. At field H_2, the magnetic moments of both the FM layers are aligned antiparallel to each other as shown by the simulated pattern in Fig. 4(c). This figure indicates the magnetic moments of thick layer pointing in the direction of the applied field and that of the thin layer in the antiparallel direction confirms the antiferromagnetic coupling between the FM layers in the PSV. The antiferromagnetic alignment between the FM layers remained when the field is increased from H_2 to H_3. At H_3 nucleation of the vortex states in the thicker layer starts as shown in Fig. 4(d). Complete formation of vortex states in thick layer and *c*-states in thin layer takes place at H_4 as shown in Fig. 4(e). The formation of the vortex and *c*-states decreases the magnetization abruptly between H_3 and H_4. At remanence (H_5) the vortex and *c*-states move toward the center of the ellipse as shown in Fig. 4(f). Propagation of the vortex and *c*-states in the ellipse occurs between H_5 and H_6, as shown in Fig. 4(g). The annihilation of the vortex and *c*-states takes place at H_7. Figure 4(h) shows the saturated states of the FM layers in the positive field direction.

C. Effect of temperature

In order to understand the variation in the interlayer coupling with temperature, magnetization measurements were performed systematically in the temperature range from 5 to 300 K for the ferromagnetically coupled (t_{Cu}=2 nm) and antiferromagnetically coupled (t_{Cu}=20 nm) samples. Figure 5 shows the representative magnetic hysteresis loops as a

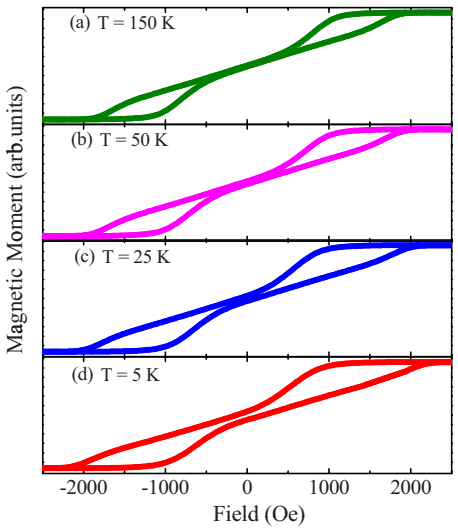

FIG. 5. (Color online) Magnetization loops of $Co_{50}Fe_{50}$(60 nm)/Cu(2 nm)/$Co_{50}Fe_{50}$(10 nm)/Cu(5 nm) elliptical nanomagnets as a function of temperature.

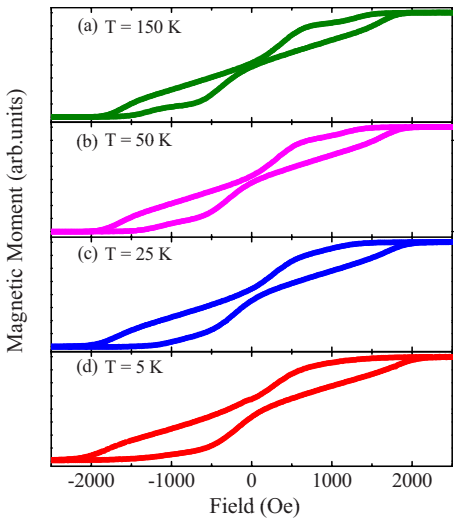

FIG. 7. (Color online) Magnetization loops of $Co_{50}Fe_{50}$(60 nm)/Cu(20 nm)/$Co_{50}Fe_{50}$(10 nm)/Cu(5 nm) elliptical nanomagnets as a function of temperature.

function of temperature for the $Co_{50}Fe_{50}$(60 nm)/Cu(2 nm)/$Co_{50}Fe_{50}$(10 nm)/Cu(5 nm) PSV. The loop at room temperature is shown in Fig. 3(a) and the loops at other temperatures are close to their nearest temperature. We observed clearly that the coupling mechanism is strongly dependent on temperature as shown by the *M-H* loops. The apparent increase in the coercive field with reducing temperature clearly indicates the resistance to the vortex displacement due to the presence of an energetic barrier. At low temperature, the edge roughness of the nanomagnets and the local anisotropy strength distribution would result in the local domain wall pinning. Similar observation was reported in $Ni_{80}Fe_{20}$ dot arrays by Shima *et al.*[27] The saturating field of the PSV increased exponentially with decreasing temperature as shown in Fig. 6. The increase in the saturating field with decreasing temperature indicates the increase in the coupling strength.

Figure 7 shows the magnetic hysteresis loop variation at selected temperatures for $Co_{50}Fe_{50}$(60 nm)/Cu(20 nm)/$Co_{50}Fe_{50}$(10 nm)/Cu(5 nm) PSV. The variation in the loop at 150 K [Fig. 7(a)] is similar to the loop variation at room temperature as shown in Fig. 3(d), indicating the antiferromagnetic coupling between the two FM layers. As the temperature decreases, the curvature of the two step reversal decreases at 50 K as shown in Fig. 7(b). For temperatures below 50 K the curvature of the two step reversal is almost diminished. Figures 7(c) and 7(d) show the variation in the magnetization at 25 and 5 K, respectively. The decrease in the curvature with temperature indicates the change in the coupling from antiferromagnetic to FM. Similar to the t_{Cu} =2 nm PSV, the saturating field increased with decreasing temperature as shown in Fig. 6. However, in the present case, the change in the sign of the coupling from antiferromagnetic to FM at low temperatures could be due to the slight increase in the saturation magnetization of the $Co_{50}Fe_{50}$ layers.[14,28] The increase in magnetization at low temperatures makes the coupling between the FM layers as FM through Néel's orange peel coupling.

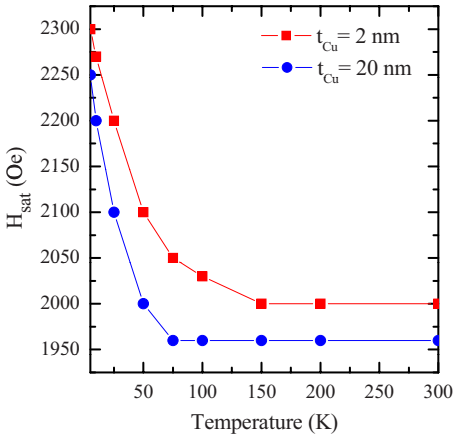

FIG. 6. (Color online) Variation in saturation field with temperature for PSV nanomagnets of Cu spacer layer thicknesses of 2 and 20 nm.

IV. SUMMARY

A systematic study of magnetization reversal in elliptical nanomagnets of $Co_{50}Fe_{50}$ films and $Co_{50}Fe_{50}$(60 nm)/Cu/$Co_{50}Fe_{50}$(10 nm)/Cu(5 nm) PSVs were performed. The effect of $Co_{50}Fe_{50}$ film thickness on elliptical nanostructures reveals that the reversal occurs via coherent spin rotation in 10 nm film and through vortex formation and annihilation in the case of 60 nm film. In the case of PSV nanomagnets, the variation in the *M-H* loop with the thickness of the Cu spacer shows a transition of the IEC from FM to antiferromagnetic at low fields for t_{Cu}=20 nm. This occurs due to the spin reversal of the thin $Co_{50}Fe_{50}$ layer to decrease the magnetostatic energy of the system. The increase in the coercive field with reduced temperature can be attributed to the pinning of the magnetic vortex. The temperature variation in *M-H* loops also revealed a change in the sign of the coupling from antiferromagnetic to FM at low temperature can be attributed to the increase in the magnetization values of the $Co_{50}Fe_{50}$ layers.

ACKNOWLEDGMENTS

The authors would like to thank Dr N. Singh from the A*Star Institute of Microelectronics, Singapore for the fabrication of templates. This work was supported by the National Research Foundation, Singapore, Grant No. NRF-G-CRP 2007-05.

[1]R. P. Cowburn, J. Magn. Magn. Mater. **242–245**, 505 (2002); A. O. Adeyeye, S. Goolaup, and N. Singh, in *Magnetic Properties of Laterally Confined Nanometric Structures*, edited by G. Gubbiotti (Transworld Research Network, Kerala, India, 2006), pp. 1–23.
[2]M. Hehn, K. Ounadjela, J. P. Bucher, F. Rousseaux, D. Decanini, B. Bartenlian, and C. Chappert, Science **272**, 1782 (1996).
[3]J. Shi, S. Tehrani, and M. R. Scheinfein, Appl. Phys. Lett. **76**, 2588 (2000); D. Goll, G. Schütz, and H. Kronmüller, Phys. Rev. B **67**, 094414 (2003); D. K. Koltsov and M. E. Welland, J. Appl. Phys. **94**, 3457 (2003).
[4]S. Goolaup, A. O. Adeyeye, and N. Singh, Phys. Rev. B **73**, 104444 (2006).
[5]R. P. Cowburn, D. K. Koltsov, A. O. Adeyeye, and M. E. Welland, Europhys. Lett. **48**, 221 (1999).
[6]P. Vavassori, O. Donzelli, L. Callegaro, M. Grimsditch, and V. Metlushko, IEEE Trans. Magn. **36**, 2993 (2000).
[7]P. Vavassori, N. Zaluzec, V. Metlushko, V. Novosad, B. Ilic, and M. Grimsditch, Phys. Rev. B **69**, 214404 (2004).
[8]T. Shinjo, T. Okuno, R. Hassdorf, K. Shigeto, and T. Ono, Science **289**, 930 (2000); M. Natali, I. L. Prejbeanu, A. Lebib, L. D. Buda, K. Ounadjela, and Y. Chen, Phys. Rev. Lett. **88**, 157203 (2002).
[9]N. Singh, S. Goolaup, W. Tan, A. O. Adeyeye, and N. Balasubramaniam, Phys. Rev. B **75**, 104407 (2007).
[10]J. C. S. Kools, T. G. S. M. Rijks, A. E. M. De Veirman, and R. Coehoorn, IEEE Trans. Magn. **31**, 3918 (1995).
[11]S. S. P. Parkin, N. More, and K. P. Roche, Phys. Rev. Lett. **64**, 2304 (1990).
[12]W. R. Bennett, W. Schwarzacher, and W. F. Egelhoff, Jr., Phys. Rev. Lett. **65**, 3169 (1990); S. S. P. Parkin, R. Bhadra, and K. P. Roche, *ibid.* **66**, 2152 (1991).
[13]E. Popova, N. Keller, F. Gendron, C. Tiusan, A. Schuhl, and N. A. Lesnik, Appl. Phys. (Berlin) **91**, 112504 (2007).
[14]J.-H. Hsu, Z.-L. Xue, and D. Sahu, J. Appl. Phys. **101**, 09D114 (2007).
[15]L. Zarate, C. Quiros, M. Velez, G. Rodriguez-Rodriguez, J. I. Martin, and J. M. Alameda, Phys. Rev. B **74**, 014414 (2006).
[16]K. S. Buchanan, K. Y. Guslienko, A. Doran, A. Scholl, S. D. Bader, and V. Novosad, Phys. Rev. B **72**, 134415 (2005).
[17]G. Gubbiotti, M. Madami, S. Tachhi, G. Carlotti, and T. Okuno, Phys. Rev. B **73**, 144430 (2006).
[18]D. V. Berkov and N. L. Gorn, J. Appl. Phys. **103**, 053908 (2008).
[19]F. J. Castaño, Y. Hao, C. A. Ross, B. Vögeli, H. I. Smith, and S. Haratani, J. Appl. Phys. **91**, 7317 (2002); X. Zhu, P. Grütter, Y. Hao, F. J. Castaño, S. Haratani, C. A. Ross, B. Vögeli, and H. I. Smith, *ibid.* **93**, 1132 (2003); C. A. Ross, F. J. Castaño, E. Rodriguez, S. Haratani, B. Vögeli, and H. I. Smith, *ibid.* **97**, 053902 (2005).
[20]D. J. Smith, R. E. Dunin-Borkowski, M. R. McCartney, B. Kardynal, and M. R. Scheinfein, J. Appl. Phys. **87**, 7400 (2000); R. E. Dunin-Borkowski, M. R. McCartney, B. Kardynal, S. S. P. Parkin, M. R. Scheinfein, and D. J. Smith, J. Microsc. **200**, 187 (2000).
[21]N. Singh, S. Goolaup, and A. O. Adeyeye, Nanotechnology **15**, 1539 (2004).
[22]E. C. Stoner and E. P. Wohlfarth, Philos. Trans. R. Soc. London, Ser. A **240**, 74 (1948).
[23]R. P. Cowburn, D. K. Koltsov, A. O. Adeyeye, M. E. Welland, and D. M. Tricker, Phys. Rev. Lett. **83**, 1042 (1999).
[24]OOMMF is available at http://math.nist.gov.
[25]B. D. Cullity, *Introduction to Magentic Materials* (Addison-Wesley, Reading, MA, 1972), p. 529; S. B. Choe, Y. Acremann, A. Scholl, A. Bauer, A. Doran, J. Stohr, and H. A. Padmore, Science **304**, 420 (2004).
[26]R. E. Dunin-Borkowski, M. R. McCartney, B. Kardynal, and D. J. Smith, J. Appl. Phys. **84**, 374 (1998); M. El-Hilo, *ibid.* **84**, 5114 (1998); M. Hwang, M. C. Abraham, T. A. Savas, H. I. Smith, R. J. Ram, and C. A. Ross, *ibid.* **87**, 5108 (2000).
[27]H. Shima, V. Novosad, Y. Otani, K. Fukamichi, N. Kikuchi, O. Kitakamai, and Y. Shimada, J. Appl. Phys. **92**, 1473 (2002).
[28]N. Persat and A. Dinia, Phys. Rev. B **56**, 2676 (1997).